

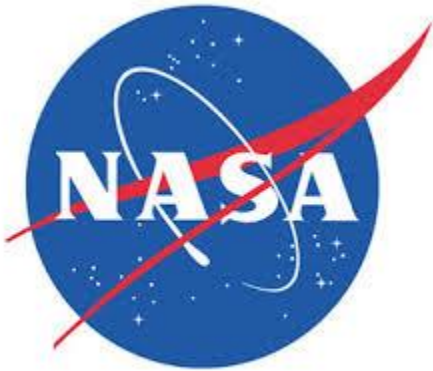
Deliverable #4: Midterm Report

EML4551C-Senior Design Fall 2013

Team 20- Direct Drive Solar-Powered Arcjet Thruster

Sponsor: Kurt Polzin (NASA)

Faculty Advisor: Wei Guo, Kwan Bing, Petru Andrei



Group Members

Christopher Brolin

Cory Gainus

Gerard Melanson

Tara Newton

Griffin Valentich

Shane Warner

Table of Contents

1.0 Abstract	1
2.0 Project Overview	1
2.1 Customer/Sponsor Requirements.....	1
2.2 Scope.....	1
2.3 Goal.....	1
2.4 Objectives.....	2
2.5 Constraints.....	2
3.0 Design and Analysis	2
3.1 Functional Analysis.....	2
3.1.1 Mechanical.....	2
3.1.1.1 Gas Valve Regulator.....	2
3.1.1.2 Thruster Housing.....	2
3.1.1.3 Anode/Cathode Spacing.....	2
3.1.1.4 Nozzle.....	3
3.1.1.5 Vacuum Chamber.....	3
3.1.2 Electrical.....	3
3.1.2.1 Circuit.....	3
3.1.2.2 Magnet.....	3
3.2 Design Concepts.....	3
3.2.1 Mechanical.....	3
3.2.1.1 Design #1.....	3
3.2.1.2 Design #2.....	4
3.2.1.3 Design #3.....	4
3.2.2 Electrical.....	5
3.2.2.1 Circuit.....	5
3.2.2.2 Magnets.....	7
3.3 Evaluation of Designs.....	8
4.0 Procurement	9
5.0 Conclusions	10
6.0 Gantt Chart	11
7.0 References	12
8.0 Appendix	13
8.1 Designed Components Details and Specs.....	13
8.1.1 Mechanical.....	13

8.1.2 Electrical 13

8.2 Detailed Analysis, Computations 14

3.2.1 Mechanical 14

3.2.2 Electrical 15

1.0 Abstract

The importance of long term control of satellite and spacecraft systems provides an opportunity for advancement in existing propulsion technologies. For the scope of this project, a solar powered arcjet thruster must be designed that eliminates the necessity of a power processing unit (PPU). Currently, startup of the thruster is achieved by transforming solar power to a desirable voltage and current via the PPU. Lighter, more affordable arcjet systems can be sent into space if this PPU is eliminated and, instead, directly driven by the solar panels. This increases the efficiency of the thruster as one of the components that fails most often is the PPU as a result of overheating. One topic under examination is the amount of thrust that can be generated without this PPU, in so-called “direct drive mode”. Reduced cost of a system that provides low thrust but high specific impulse in this manner could greatly improve the functionality of thrusters used in space.

2.0 Project Overview

2.1 Customer/Sponsor Requirements:

- Produce a high voltage-pulse that can breakdown the injected gas to cause ionization.
- Design a scalable arcjet thruster capable of processing 50-400W of power without the use of a power processing unit.
- Design a vacuum chamber in order to properly simulate the space environment for testing the thruster.
- Design and execute a test/experiment in order to determine the thruster’s range of operating conditions over which the ionization or gas breakdown will occur.
- Perform a successful test to quantify the conditions over which a continuous discharge at the given power levels can be sustained.
- Determine if this continuous discharge is possible within the range of conditions provided by the solar panels

2.2 Scope:

The project scope is to design, fabricate, and test an electric arcjet thruster within a vacuum chamber that will be designed to simulate the space environment at which the thruster will operate. The arcjet thruster will operate on a direct drive system eliminating the need for a power processing unit (PPU), thereby reducing the weight of the system, its complexity, and most importantly cost while maintaining efficiency. The use of solar panels as the arcjet’s source of energy will be used since the abundance of solar energy is present in the space environment.

2.3 Goal:

To successfully design and test an arcjet thruster within a vacuum chamber that meets all of our customer’s requirements.

2.4 Objectives:

- Operate on direct drive by eliminating the PPU
- Generate an arc capable of breaking down a gas propellant
- Produce a current density that will sustain the plasma
- Produce a model that is scalable for NASA applications
- Design and build a reliable test model
- Create a space-like test environment
- Create and carry out an experiment to determine the amount of thrust produced

2.5 Constraints:

- Work within our budget of \$500
- Time constraints of deliverables
- Minimize weight
- Set input power source (Solar arrays provided by NASA)
- Produce a pressurized gas within a vacuum environment

3.0 Design and Analysis

3.1 Functional Analysis

3.1.1 Mechanical

3.1.1.1 Gas Valve Regulator

The gas valve regulator will be provided by the manufacturer of the argon gas tank and will function as a control valve to regulate the flow of argon gas into the thruster.

3.1.1.2 Thruster Housing

The thruster housing will function as the body of the thruster which houses some of the major components such as the annular anode, cathode, and magnets. The housing will also function as a control volume by containing the argon gas in order to allow for the plasma to be created.

3.1.1.3 Anode/Cathode Spacing

The anode and cathode spacing within the thruster housing will function as a major component in the arcjet thruster. The spacing between the anode and cathode is important because it determines the breakdown voltage needed to ionize the argon gas.

3.1.1.4 Nozzle

The converging-diverging nozzle within the arcjet thruster will allow the argon ions generated by the arc to be accelerated past sonic velocity. The nozzle will also function with the help of magnets to contain the plasma at a centerline off the walls of the nozzle.

3.1.1.5 Vacuum Chamber

The vacuum chamber will be used to house the arcjet thruster in order to conduct a proper experiment simulating the space environment, where the arcjet thruster will be used.

3.1.2 Electrical

3.1.2.1 Circuit

The circuit will consist of solar panels, an inductor, an IGBT, pulse generator, and a potentiometer. The solar panels will provide electrical energy to the circuit and ionization process. The circuit must be capable of producing a voltage spike ranging from 137 V to 1.034 kV. Once the system is in steady state the current through the plasma (anode/cathode) should be approximately 5.5 A.

3.1.2.2 Magnets

The magnet is needed to direct flow of the plasma through the nozzle, protect the thruster from overheating, and help produce additional thrust.

3.2 Design Concepts

3.2.1 Mechanical

3.2.1.1 Design #1

The first design considered for this project was the baseline design produced by former NASA intern Nicholas Rongione. A schematic of this design is shown in Figure 4.

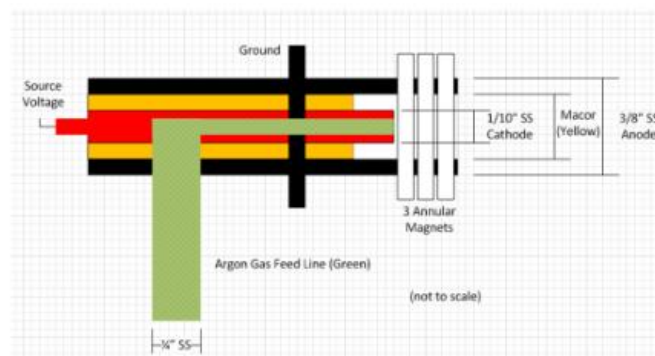


Figure 4

This design is characterized by a large cylindrical stainless steel tube acting as the anode, with a smaller stainless tube acting as the cathode. Both are along the same centerline axis. The argon gas enters into the housing and is injected directly into the cathode. The gas exits the cathode into a constant area nozzle surrounded by three annular magnets that directs the flow of the argon ions out of the nozzle, and protect the nozzle/anode walls from the high temperature fluid. The cathode is also insulated with Macor to prevent a short of the circuit.

3.2.1.2 Design #2

The next design improves upon Design 1 in that it utilizes a converging-diverging nozzle in order to help accelerate the flow of the argon gas passed sonic velocity. Rather than injecting the argon gas directly through the cathode, this design injects the gas into the thruster housing perpendicular to the cathode. This design concept is depicted in Figure 5.

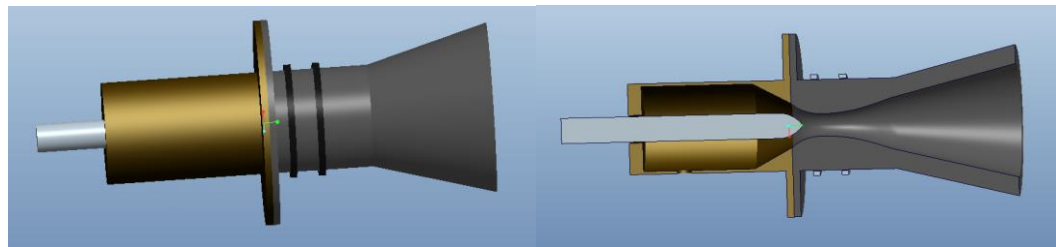


Figure 5

The converging diverging nozzle acts as the anode and the cylindrical rod with a pointed tip acts as the cathode. The magnets are placed around the front side of the nozzle and are represented as the rings in Fig. 5. The placement of the magnets will help confine the high temperature argon ions away from the surface of the nozzle and will help direct the flow downstream to the nozzle exit.

3.2.1.3 Design #3

The final arcjet thruster design is similar to Design 2 in that the argon gas is not directly injected into the cathode. Instead of injecting the gas into the housing perpendicular to the cathode, this design has the argon gas being injected into the housing at an angle. The reason for injecting the argon gas at angle is to create a convective flow of the argon gas that will help cool the cathode by creating a boundary layer. The CAD model of this design is shown in Figure 6.

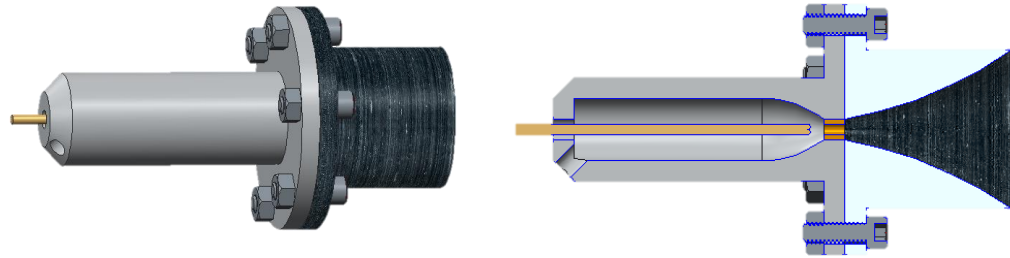


Figure 6

This design utilizes a cylindrical housing with the end of it acting as the converging portion of the converging diverging nozzle. The long cylindrical rod that is located along the centerline axis of the cylindrical housing is the cathode. The hole on the front side of the housing near the entrance of the cathode is angled in order to allow for the argon gas to be pumped into the housing as previously discussed. The anode is located at the end of the cylindrical housing inside the throat of the converging diverging nozzle. This will ensure that the arc between the cathode and anode will be generated when the argon gas is choked to sonic velocity. After the arc is produced the argon gas becomes ionized and is accelerated past sonic velocity. The argon ions are able to accelerate by increasing the area of the nozzle shown in Fig. 6 in the diverging portion. In order to attach the housing to the diverging portion of the nozzle, flanges are incorporated into the design of both parts. This will allow for ease of mating and securing the two parts together with the use of screws and nuts.

3.2.2 Electrical

3.2.2.1 Circuit

When the thruster is constructed, the actual anode/cathode spacing and pressure of Argon isn't accurately known. Since the breakdown voltage depends on the product of the pressure and anode/cathode distance, it is desired we design a circuit that can adjust the breakdown voltage to match the product of the pressure and distance. There are three different designs we could use to implement these requirements. The first design would be a power processing unit that converts the voltage and current to the proper value for thruster operation. The sponsor specifically asked us to replace this to make the system more efficient so that rules out that option. Another possible design is to create a voltage spike with a capacitive circuit, but the voltage across a capacitor does not change instantaneously, so that would be difficult to do. A better design is to use an inductive circuit to create a voltage spike because the current through an inductor does not change instantaneously, however the voltage can. This is given by $V = L \frac{di}{dt}$, where di is the change in current, dt is the time it takes for the circuit to open, L is the inductance,

and V is the voltage across the inductor. A functional schematic is shown in Figure 7. A potentiometer in place of R_2 is capable of adjusting the voltage spike, because steady state current will drop to zero in the amount of time it takes the IGBT to open, thus a potentiometer could control the di term, which controls the voltage spike.

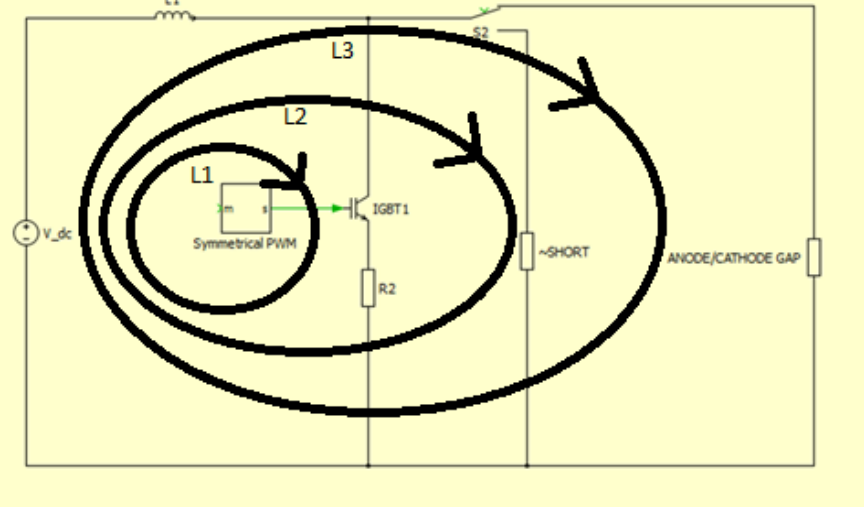


Figure 7

In order to start up the thruster, the IGBT in Fig. 7 will be closed by a simple selector switch that provides enough voltage to close the IGBT. When the IGBT is closed, loop L1 will conduct current, while loop L2 and L3 will be open circuits. The time it takes L1 to reach steady state is given by $5 \times \tau = 5 \times \frac{L}{R_2}$. We plan to use a potentiometer for R_2 that ranges from 14Ω to 105Ω , and inductance of $47 \mu\text{H}$, thus τ ranges from $0.448 \mu\text{s}$ to $3.36 \mu\text{s}$. When loop L1 reaches steady state the current will be $I_1 = \frac{V_{dc}}{R_2}$, where V_{dc} is the voltage supply from the solar panel, thus I_1 will range from 0.733 A to 5.5 A . When the selector switch is opened the IGBT will open, hence every loop in Fig. 7 will be open, but the inductor will react strongly because the current through an inductor doesn't change instantaneously given by $V = L \frac{di}{dt}$, where dt is the IGBT flip time approximately 250 ns , $L = 47 \mu\text{H}$, $di = I_1 - 0$, hence V will range from 137 V to 1.034 kV . This breakdown voltage will create an arc across the anode/cathode gap shown in loop L3, which ionizes the argon flowing through the gap and produces a plasma. Immediately after the arc, current will flow through the plasma, which will act as a resistance that is thought to be very small, hence current will flow through the ~SHORT resistor shown in Fig. 7, loop L2.

3.2.2.1 Magnets

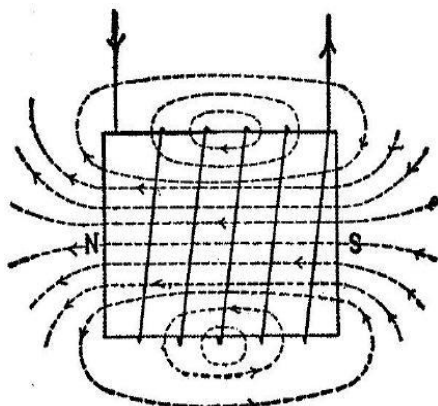


Fig. 145. DIAGRAM OF AN ELECTRO-MAGNET SHOWING RELATION OF CURRENT AND WINDING TO ITS POLARITY AND LINES OF FORCE.

Figure 8

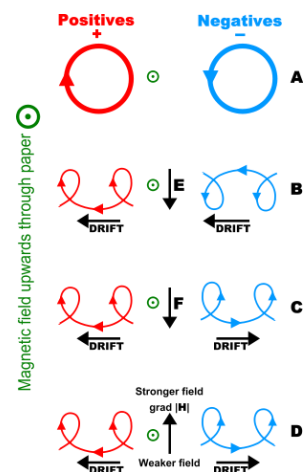


Figure 9

The magnet will be placed around the nozzle in order to keep the plasma off the walls of the nozzle and will confine the plasma to a certain radius. It also helps increase thrust. Figure 8 depicts an electro-magnet that can be replaced by a bar magnet with the same characteristics. One could imagine a plume of positive and negative charges due to the ionization of Argon through the anode/cathode. This plume wants to expand outward but the magnet is pushing the charges of the plume inward causing the charges to move in a helical path as shown in Figure 9. The magnetic field at which we can confine the negative and positive charges in a bar magnet is given by $B = \frac{mv}{qr}$, where m is mass, v is velocity, q is charge, r is radius, and B is the magnetic field. For now we approximate the strength of the magnet to be $B = 1 \text{ mT}$, but we must further research the velocity of the charges to get an accurate calculation.

3.3 Evaluation of Designs

Table 1: Decision Matrix

	Weights	Design 1		Design 2		Design 3	
		Rating	Weighted Score	Rating	Weighted Score	Rating	Weighted Score
Life Expectancy	0.10	7	0.72	7	0.72	8	0.83
Material Cost	0.21	2	0.41	7	1.45	8	1.66
Ease of Assembly	0.10	6	0.62	8	0.83	3	0.31
Manufacturability	0.17	5	0.86	4	0.69	7	1.21
Ease of Closing Circuit	0.07	9	0.62	9	0.62	4	0.28
Temperature	0.14	8	1.10	4	0.55	9	1.24
Magnet Insertion	0.03	6	0.21	6	0.21	8	0.28
Gas Insertion	0.03	3	0.10	3	0.10	9	0.31
Reliability	0.14	2	0.28	7	0.97	8	1.10
TOTAL	1		4.93		6.14		7.21
RANK			3		2		1

The detailed matrix chart, shown in Table 1, was used as an aid in deciding which design best suited the needs of the project. Each design was measured in its ability to fulfill a total of nine different categories: life expectancy, material cost, ease of assembly, manufacturability, ease of closing the circuit, temperature, magnet insertion, gas insertion and reliability. These categories were given a weight based on the influential importance each would have on the desired final product – the sum of all categories adding up to 1, such that a weighted score could be assigned to each design. Based on the ratings given to each design, a final weighed score is established such that the higher the final total, the more desirable the design.

Designs 1 and 2 fell short for a variety of reasons. Design 1 scored low in reliability since the flow of fuel through the arc isn't maximized as it is in the other two designs. The cost of the first design is also significantly higher due to the selection of an expensive insulation material to be used between the cathode and the grounded material.

As a result of this decision matrix, Design 3 was determined to be the best option. It scored the highest in seven of the nine categories, falling short in its ease of assembly and ease of closing the circuit. This design calls for the magnet to be placed in the throat of the system, as opposed to being wrapped around the exterior of the nozzle. Thus, accurately assembling this design would be qualitatively more difficult. In addition, closing the circuit for this design would be complicated due to the position of the anode within the system.

Conversely, this design scored very high in gas insertion method and temperature control. Design 1 injects the fuel in a direction parallel to the desired thrust direction, Design 2 injects the fuel in a perpendicular direction to the cathode, while Design 3 deposits the fuel at an angle to the final flow direction. This creates swirls which aid in cooling the high temperature fuel and potentially exposing a higher percentage of gas to the electric arc.

4.0 Procurement

Table 2: Budget Analysis for Design 3

Component	Description	Quantity	Cost	Manufacturer
Cathode	Tungsten Rod, 3/16" x 6"	2	\$ 33.24	McMaster Carr
	Stainless Steel 304, 3/16" x 6'	1	\$ 9.36	McMaster Carr
Anode	Stainless Steel 304, 1 1/4" OD 3/4" ID, 1/4" Wall Thickness	1	\$ 51.51	McMaster Carr
Vacuum Chamber	Low Carbon Steel, 12" x 24', 1/4" Thick, Sheet	3	\$ 252.12	McMaster Carr
	Low Carbon Steel, 12" x 12', 1/4" Thick, Sheet	2	\$ 96.70	McMaster Carr
	Aluminum 6061, 12" x 3', 1/4" Thick, Sheet	1	\$ 63.64	McMaster Carr
	Clear Acrylic, 6" x 12", 1/4" Thick, Sheet	1	\$ 10.99	McMaster Carr
Vacuum Pump	6 CFM 2 Stage Vacuum Pump	1	\$ 266.60	ZnergyTools.com
Argon Gas Cylinder	20 CF, Welding Cylinder	1	\$ 77.00	Welding Supplies from IOC
Argon Gas	20 CF Fill	1	TBD	Depending on Regional Location
Hose	High/Pressure Vacuum Hose	1	\$ 29.17	McMaster Carr
Hose Fitting	Outlet Fitting, Right Hand Thread, Brass	1	\$ 1.23	McMaster Carr
Housing/Nozzle	Stainless Steel 304, 2' Diameter, Stock	1	\$ 56.50	McMaster Carr
O-Ring	High Temp Buna-N O-Rings, 1" OD, 3/32" Width	2	\$ 18.24	McMaster Carr
Bolts	Stainless Steel 316, Fully Threaded, 7/8" Long, 1/4"-20 Thrad	1	\$ 5.23	McMaster Carr
Nuts	Stainless Steel 18-8, Easy-On Flange Hex Locknuts, 1/4"-20 Thread	1	\$ 7.78	McMaster Carr
Insulation	Macor Rod, 1/4" Diameter, 3' Long	1	\$ 18.96	McMaster Carr
IGBT	N-Channel Enhancement, 1200 V, IC=25 A	1	\$ 21.30	Fouraker Tallahassee
Inductor	100.0 μH, 6 A	1	\$ 2.62	Digi-Key
Switch	Toggle Switch, SPDT, Item# 2TNV5	1	\$ 4.41	Grainger
Potentiometer	Part# AVT200-250-ND	1	\$ 15.62	Digi-Key
Magnet	Ceramic Ring Magnet, ID 2"	3	\$ 11.25	American Science & Surplus
		TOTAL	\$1,053.47	

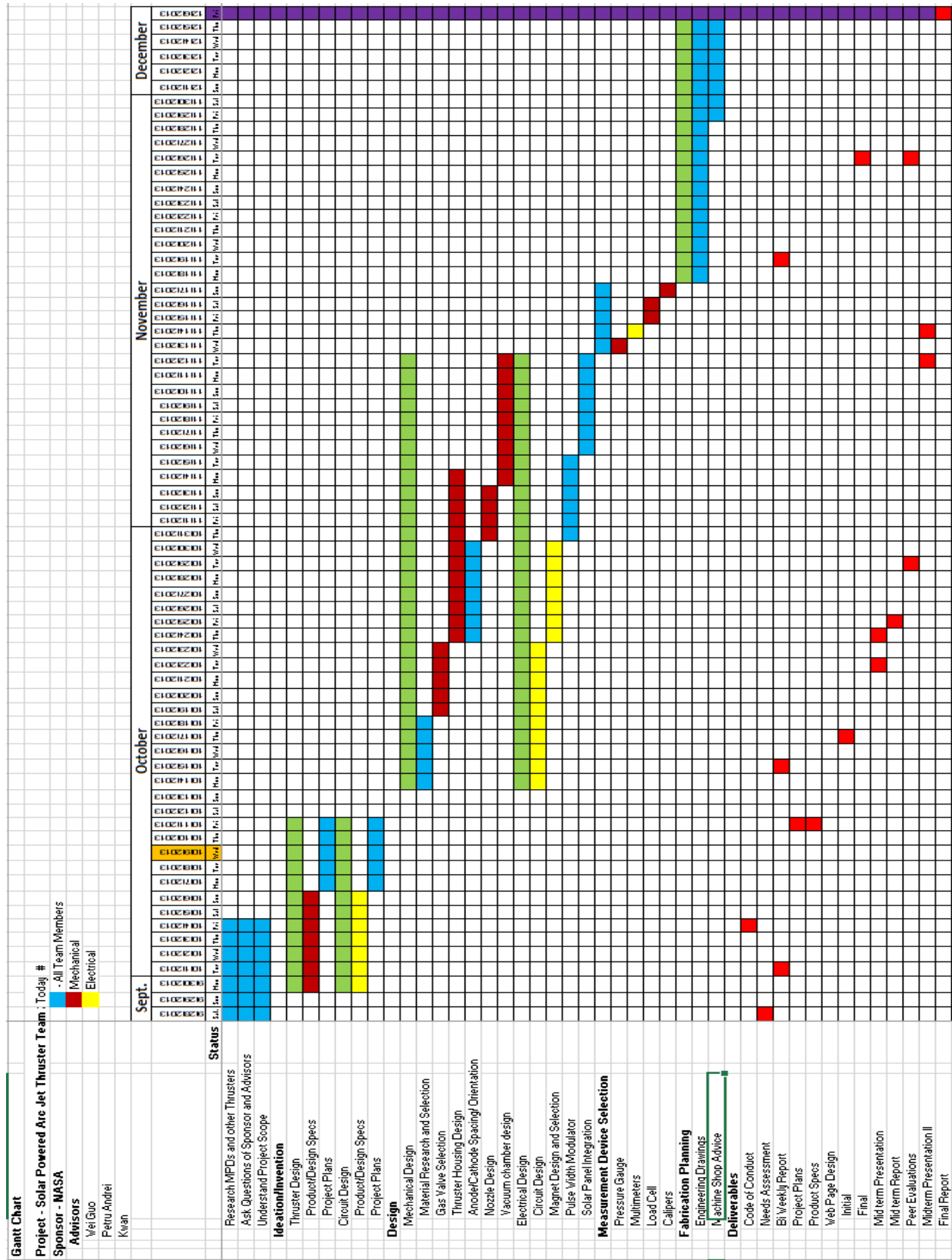
The budget allocated for our senior design project is \$500, however the total shown in our cost analysis is \$1,053.47. This total does include a vacuum pump, however this component will most likely be borrowed rather than purchased out right. After breaking down the parts we need it is necessary for us to request more funding in order to complete the project to fulfill the costumers' needs.

5.0 Conclusions

Elimination of the power processing unit as demonstrated in our choice of Design 3 would, theoretically, allow for sufficient thrust at a reduced cost for spacecraft orientation. In addition, lifetime of the system is increased since failure of PPU is no longer in consideration. Price of the general design is also significantly diminished by using direct-drive, as current designs must allocate a large portion of the budget to invest in a power processing unit.

As mentioned above, a major expenditure for the project is derived from the need to manufacture a vacuum chamber specifically for testing purposes. Had this design been implemented and tested in a facility already possessing a viable vacuum chamber, the costs of this project would be greatly reduced. Taking this into account, the overall expenses for a design such as this provides a better opportunity to meet the customer's budget of \$500.

6.0 Gantt Chart



7.0 References

- 1) Polzin, Kurt. "Senior Design Project Definition." NASA, n.d. Web. 26 Sept. 2013.
- 2) Matthew Krolak. "MPD Thruster Thesis." Worcester Polytechnic Institute, May 2007.
- 3) Nicolas Augustus Rongione. "Direct Solar Powered Arcjet Thruster (DiSPAT)" NASA, n.d. August 9, 2013.
- 4) William Anthony Hargus, Jr. "Hall Acceleration Mechanism" US Air Force Research Laboratory. March 2001
- 5) Geoff Dickinson. "Non-impulsive orbit raising using an ATOS type arcjet thruster" ASEN5050. Dec. 2002.
- 6) F. Paganucci, P. Rossetti, M. Andrenucci. "Performance of an Applied Field MPD Thruster" RIAME-MAI. 2001.

8.0 Appendix

8.1 Designed Component Details and Specs

8.1.1 Mechanical

Design #3

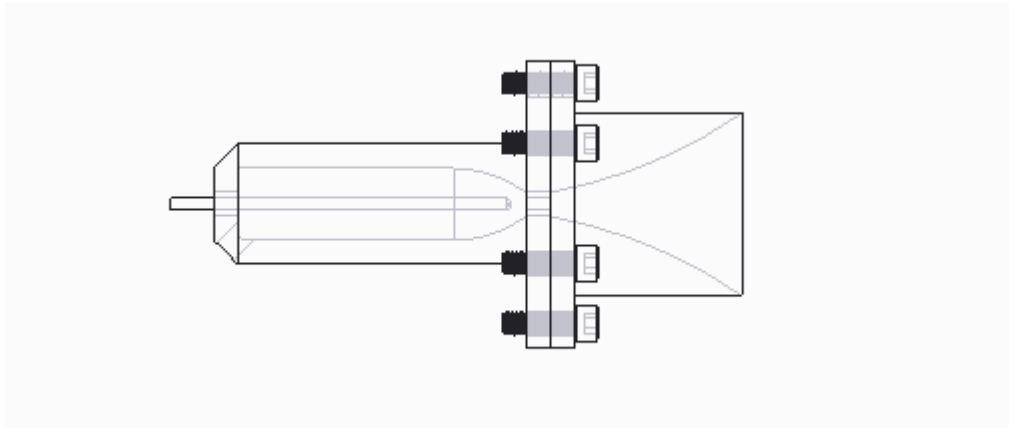


Figure 10

*Above is a rough schematic of the design to be used, however the exact dimensions have not been chosen yet.

8.1.2 Electrical

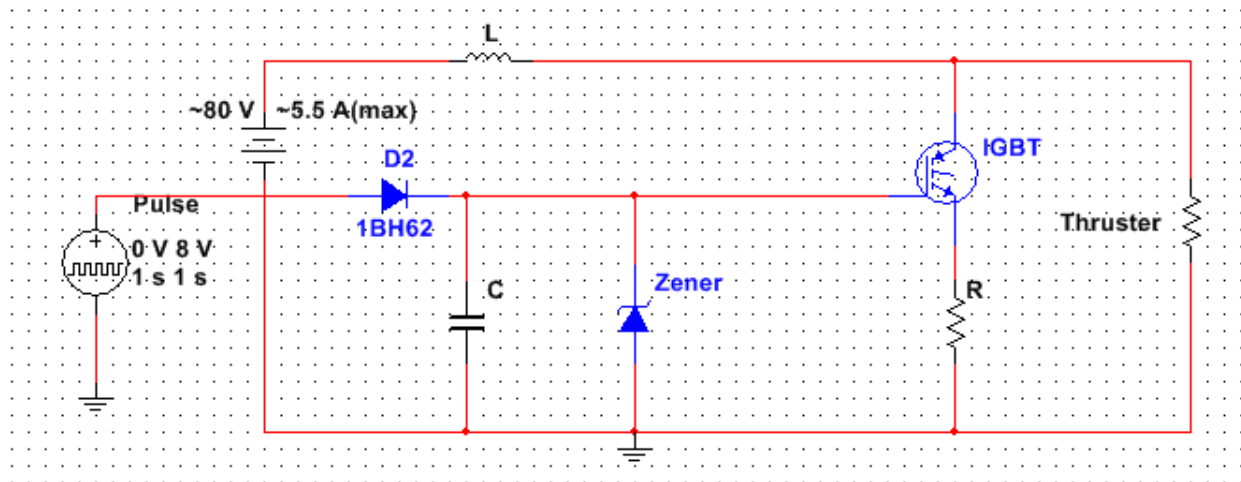


Figure 11

Figure 11 is a detailed design of a functional circuit that meets the requirements. The magnet design will look similar to fig. 8.

8.2 Detailed Analysis, Computations

8.2.1 Mechanical

```
%Feed Calculations

P_o = [2500:-1:500]; % Stagnation Pressure in the Cylinder (psi)
P_o2 = P_o.*6894.76; % Stagnation Pressure in the Cylinder (Pa)

P_g = 20; % Static Pressure leaving Cylinder (psi)
P_g2 = P_g*6894.76; % Static Pressure leaving Cylinder (Pa)

rho_argon = 1.784; % kg/m^3
D_feed_tube = 0.25*0.0254; % Diameter of the Gas feed tube in (m)

D_Throat = 0.75*0.0254; % Diameter of nozzle throat (m)
A_Throat = (3.1416/4).*(D_Throat.^2);
P_c = 245.31:.3773:1000; % Ionization Chamber Pressure (Pa)
d = 0.00381; % Anode-Cathode distance (m)
P_v = (1*10^-4)*133.322368; % Ambient Pressure of Vacuum Chamber (Pa)

% Canister to Feed Tube
V_g = sqrt(2*rho_argon.*(P_o2 - P_g2));%m/s
m_dot_Ar = V_g.*(rho_argon*3.1416*((D_feed_tube)^2)/4); % kg/s

% Feed tube to Ionization Chamber
V_c = sqrt((P_g2 - P_c) + (0.5*rho_argon.*V_g.^2).*(2*rho_argon)); %m/s
A_Ion = m_dot_Ar./(V_c.*rho_argon); %m^2
V_Ion = A_Ion.*(8*.0254); % Volume of the Ionization Chamber

% Velocity Exiting the throat
V_v = sqrt((P_c - P_v) + (0.5*rho_argon.*V_c.^2).*(rho_argon*2)); %m/s
m_dot_exit = V_v.*(rho_argon.*A_Throat);% kg/s
%A_Throat = m_dot_Ar./(V_v.*rho_argon); % m^2

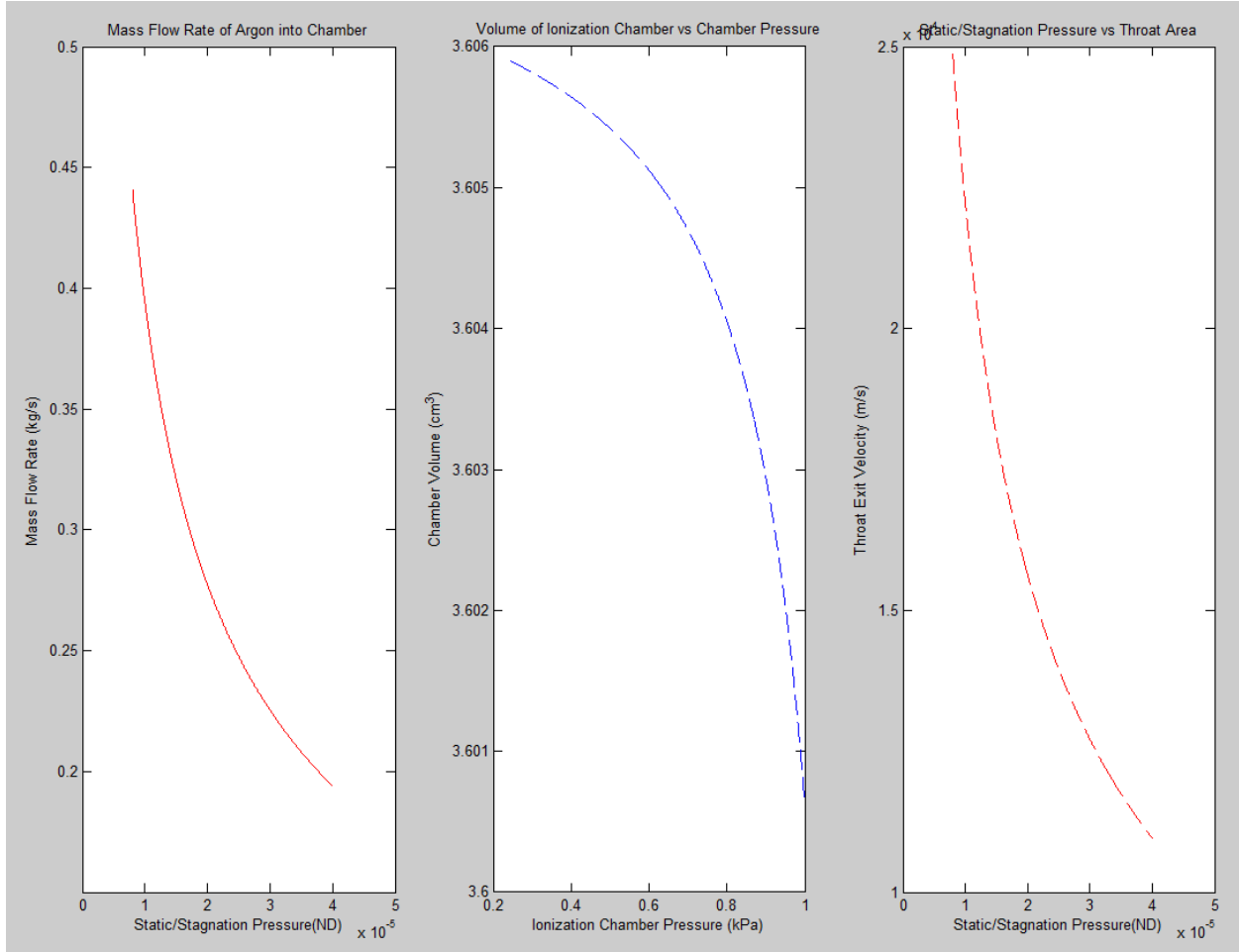
subplot(1,3,1)
plot((P_g2./P_o2)./1000,m_dot_Ar, 'r')
title('Mass Flow Rate of Argon into Chamber')
xlabel('Static Pressure/Stagnation Pressure in Feed Tube (ND)')
ylabel('Mass Flow Rate (kg/s)')

subplot(1,3,2)
plot(P_c./1000,V_Ion.*(100^3), '--b')
title('Volume of Ionization Chamber vs Chamber Pressure')
xlabel('Ionization Chamber Pressure (kPa)')
ylabel('Chamber Volume (cm^3)')
```

```

subplot(1,3,3)
plot((P_g2./P_o2)./1000,V_v,'--r')
title('Static/Stagnation Pressure vs Exit Velocity ')
xlabel('Static/Stagnation Pressure (ND) ')
ylabel('Throat Exit Velocity (m/s) ')

```



8.2.2 Electrical

For the magnet we calculated the magnetic field with $B = \frac{mv}{qr}$, $v = \sqrt{\frac{20eV}{3m}}$. These equations simplify to give us $B = 2.889/r$ mT.

As described in section 3.2.2.1, the inductor of figure 11 will be capable of producing a voltage spike of magnitude $V = L \frac{di}{dt}$, where $dt = 250$ ns, $L = 47$ μ H, $di = 5.5_{\max}$ or 0.733_{\min} A, thus the breakdown voltage will range from 137 V to 1.034 kV.